Single-atom nanozymes-based catalytic ROS clearance for efficient alleviating eczema

Zhen Wan,‡[a,b] Yadong Zhe,‡[a] Jiarong Li,‡[c] Qingshan Liu,[a] Danqi Ding,[c] Shaofang Zhang,[a] Shuangjie Liu,[a] Hao Wang,[a] Jiang Yang,[d] Xin Sun, [a] Huanhuan Qiao[a] and Xiaoyu Mu*[a]*

[a] Tianjin Key Laboratory of Brain Science and Neural Engineering, Academy of Medical Engineering and Translational Medicine, Tianjin University, Tianjin 300072, China

[b] Haihe Hospital, Tianjin University, Tianjin300350, China

[c] Department of Physics and Tianjin Key Laboratory of Low Dimensional Materials Physics and Preparing Technology, School of Sciences, Tianjin University, Tianjin 300350, China

[d] *State Key Laboratory of Oncology in South China, Collaborative Innovation Center for Cancer Medicine, Sun Yat-sen University Cancer Center, Guangzhou 510060, China.*

‡ These authors contributed to this work equally.

1 Reagents and Characterization

Reagents

Pyrene (98%), urea (AR), ruthenium (III) chloride ($RuCl_3$, 99.95%), 3,3',5,5' tetramethylbenzidine (TMB, 98%), 5, 5-dimethyl-1-pyrrolin-N-oxide (DMPO, 97%) were purchased from Tianjin Heowns Biochem Technologies Co., Ltd. (China).Iron chloride hexahydrate (AR,$FeCl_3 \cdot 6H_2O$, 99%) and HRP (>300 U/mg) were purchased from Shanghai Macklin Biochemical Co., Ltd. (China). Nitric acid (AR, 65.0-68.0%) was purchased from Tianjin Damao Chemical Reagent Co., Ltd. (China). Deionized water (>99.5%) was purchased from Tianjin Jiangtian Chemical Technology Co., Ltd. (China). Ammonium hydroxide (28.0-30.0%) was purchased from Anhui Senrise Technology Co., Ltd. (China). H_2O_2 solution (AR, 30 wt% in H_2O) was purchased from Shanghai Aladdin Biochemical Technology Co., Ltd. (China). NADH-Na_2 (>98%). TMB substrate colorimetric reagent kit (ELISA, HRP colorimetry) was purchased from Anhui Leagene Biotechnology Co., Ltd. (China). Total SOD assay kit (NBT riboflavin colorimetric method) was purchased from Shanghai Yuanye Bio-Technology Co., Ltd. (China). Acetic acid buffer (pH 4.5) was purchased from Beijing biotopped Technology Co., Ltd. (China).

Materials characterization

The morphology and size of RuN_4-SAzyme were observed by dark-field transmission electron microscopy (TEM, JEM-F200, JEOL, Japan). Analysis of metal element content was performed using inductively coupled plasma mass spectrometry (ICP-MS:Agilent 7800, Agilent Technologies Ltd, Singapore). Atomic information of SANs was observed using aberration-corrected scanning transmission electron microscopy (AC-STEM, ARM200F, JEOL, Japan). X-ray diffraction (XRD, Smartlab, Rigaku, Japan) was employed for crystallographic identification of RuN_4-SAzyme. The Raman spectra was measured by an ultra-fast Raman imaging spectrometer (XploRA PLUS, HoribaJY, France) with the scanning wavenumber range of 500 - 3500 cm^{-1}. Elemental composition, chemical states were obtained using X-ray photoelectron spectrometer (XPS, Axis Supra, Kratos Analytical Ltd, UK). The ·OH

scavenging measurements were conducted on an ESR spectrometer (JES-FA200, JEOL, Japan).

Cell Toxicity Assessment

Rat Aortic Endothelial Cells (RAOECs) were seeded in a 96-well plate at a density of approximately 4000 cells per well using Dulbecco's Modified Eagle Medium (DMEM) and incubated at 37°C for 12 hours to allow attachment and initial growth. Subsequently, a range of RuN_4-SAzyme concentrations, from 0 to 25 μg/mL, were introduced into each well. Following an additional 24-hour incubation period, cell viabilities were assessed using the CCK-8 assay to determine the potential toxicity of the RuN_4-SAzyme solutions.

Anti-oxidative levels of RuN_4-SAzyme in vitro.

RAOECs were plated in 6-well plates at a density of 15,000 cells per well and allowed to grow until fully adherent. DMEM containing RuN_4-SAzyme at a concentration of 12 μg/mL was added to each well, followed by the introduction of LPS at a concentration of 0.5 mg/mL. After a 6-hour incubation period, DCFH-DA and DHE reagents were incorporated into the culture medium to measure intracellular levels of total ROS, including $O_2^{\bullet-}$. Following incubation times of 20 and 30 minutes for DCFH-DA and DHE respectively, the plates were rinsed three times with PBS to terminate the reactions. The RuN_4-SAzyme served as a control in these experiments. Cellular fluorescence was visualized using a fluorescence microscope (EVOS, AMG), and quantitative analysis was conducted using flow cytometry (BD Accuri™ C6). The differences in fluorescence intensity were compared to analyze the levels of free radicals within the cells.

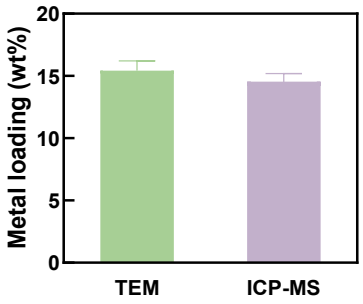

Fig. S1 Ru atoms loading by EDS and ICP-MS.

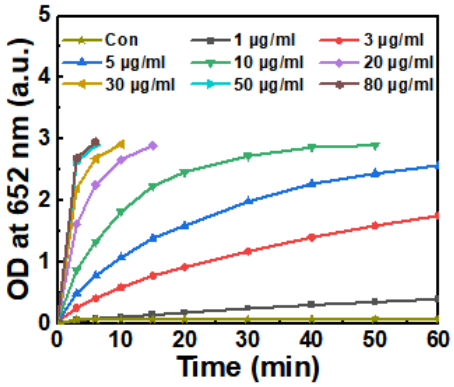

Fig. S2 Time-dependent absorbance changes of TMB for POD-like activity of RuN_4-SAzyme.

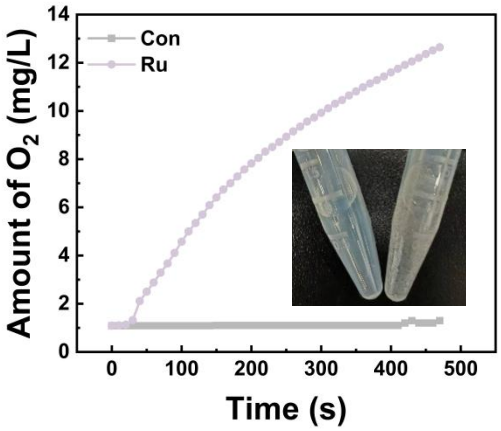

Fig. S3 Dissolved oxygen generated in H_2O_2 solutions with/without RuN_4-SAzymes (100 μg/mL). The insert image is a photograph of RuN_4-SAzyme (100 μg/mL) catalyzing the formation of oxygen bubbles in 500 mM H_2O_2 solution after incubation for 5 min.

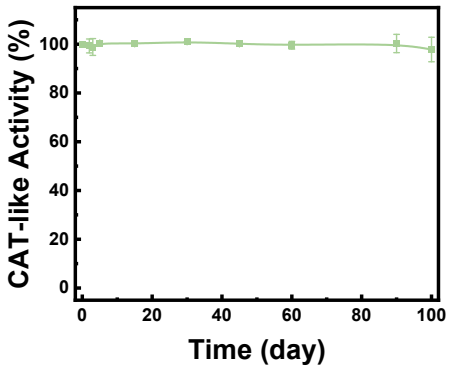

Fig. S4 The stability of CAT-like activity of RuN_4-SAzyme.

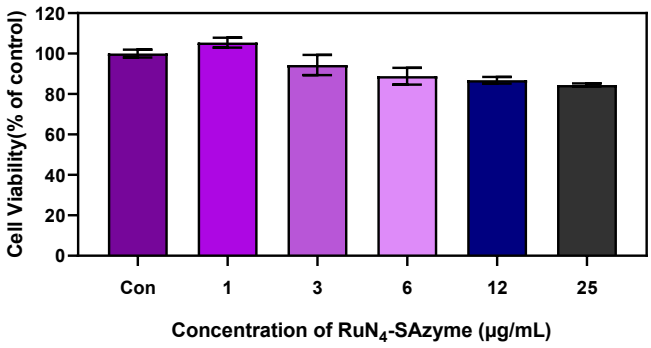

Fig. S5 Cytotoxicity of RuN_4-SAzyme on RAOECs.

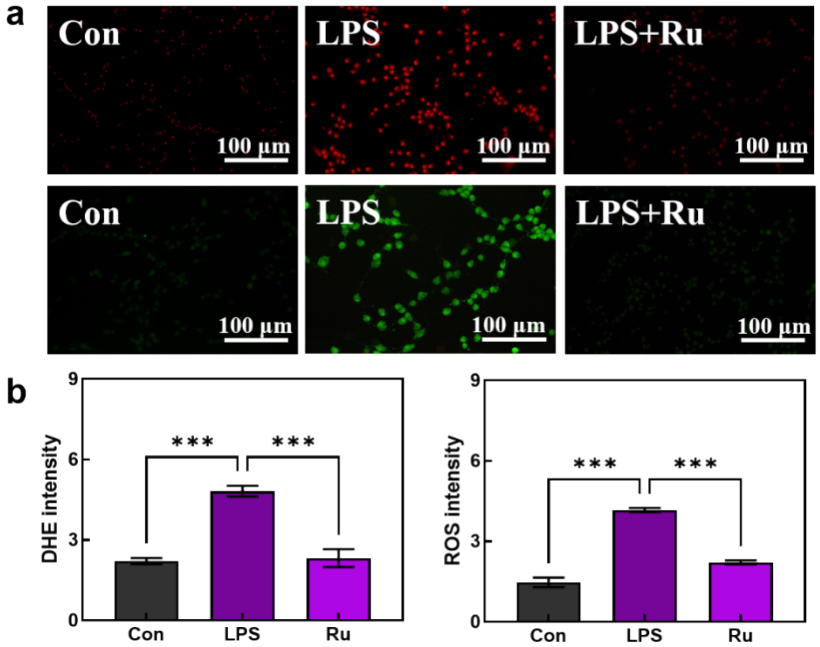

Fig. S6 Anti-oxidative levels of RuN_4-SAzyme *in vitro*. a. Total ROS and $O_2^{\bullet-}$ fluorescent staining in RAOECs induced by LPS before and after RuN_4-SAzyme treatment. b. The corresponding quantitative intensity of the total ROS and $O_2^{\bullet-}$ fluorescent staining in RAOEC cells induced by LPS before and after RuN_4-SAzyme treatment. Data are presented as means ± SEM. Asterisks indicate significant differences (*P < 0.05, **P < 0.01, ***P < 0.001) versus with the eczema group, which were analyzed by one-way analysis of variance (ANOVA) with the Tukey test.

Fig. S7 Photographs of the backs of mice with or without intervention on the second and twelfth days.

Fig. S8 H&E staining of skin with or without intervention. The area circled by the rectangular box in the figure corresponds to the enlarged view of **Figure 3e**.

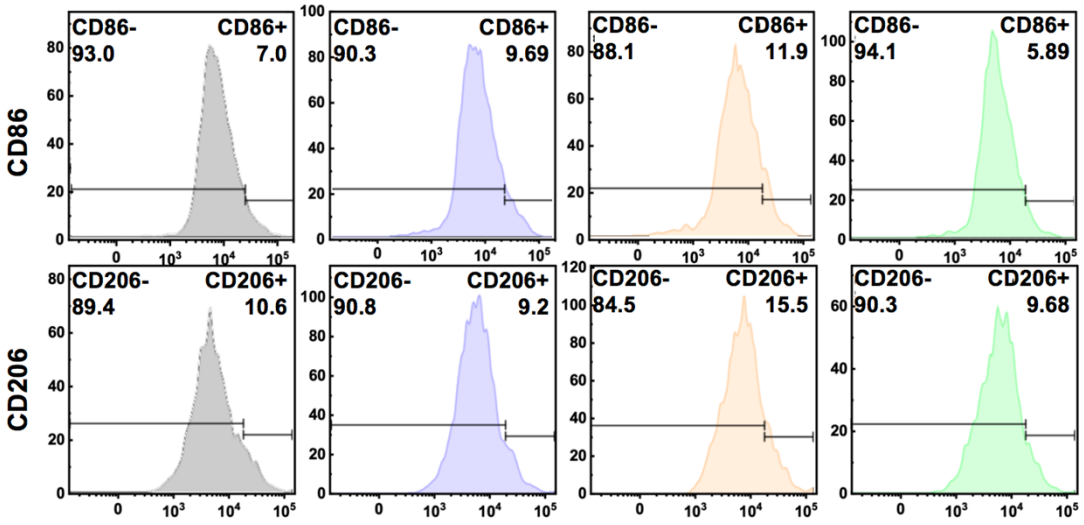

Fig. S9 Representative gating strategy for analysis of M1 and M2 macrophages about flow cytometry.

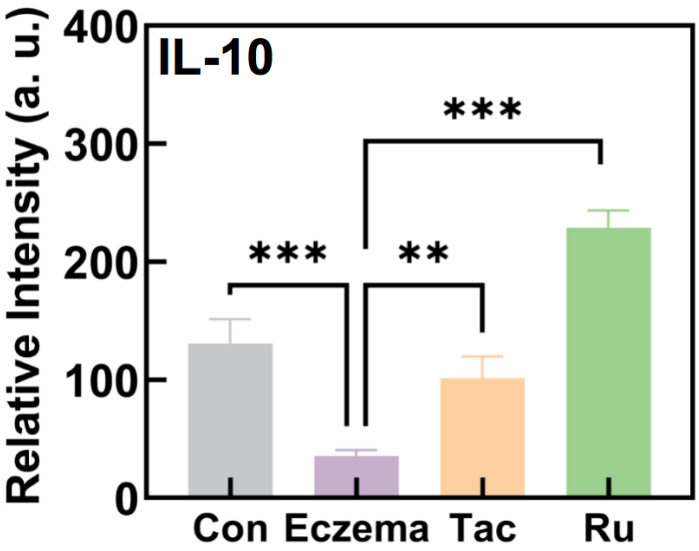

Fig. S10 Corresponding quantitative analysis of IF staining (n = 3 per group). Data are presented as means ± SEM.

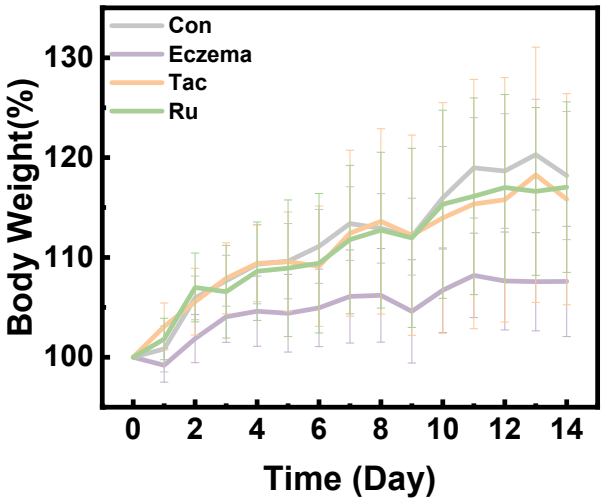

Fig. S11 Body weight changes over time in groups with or without intervention (n = 8 per group). Data are presented as means ± SEM.

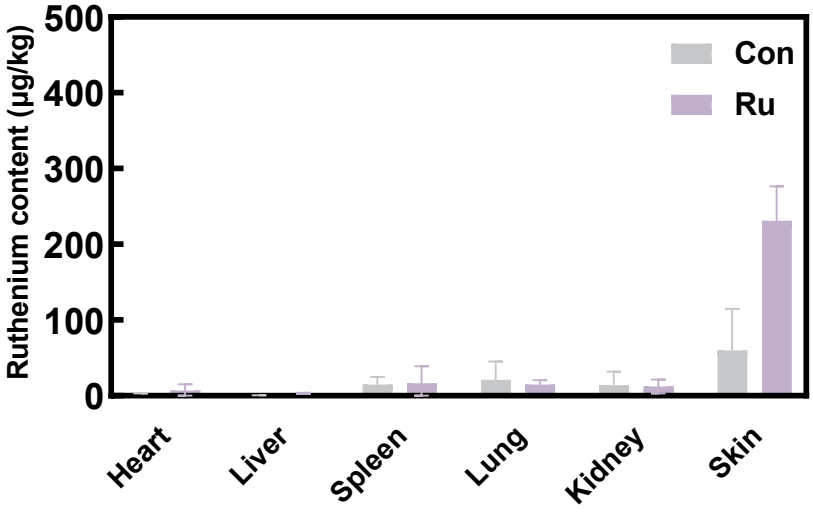

Fig. S12 Metal content in the skin and major organs (heart, liver, spleen, lung, kidney) in the RuN_4-SAzyme-treated group and Control group (*n*=3 per group).

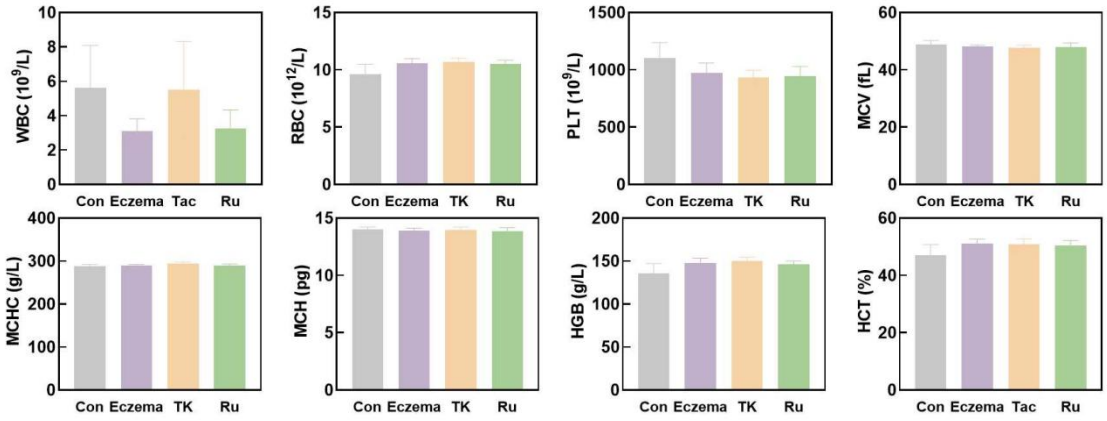

Fig. S13 Hematology data of mice in groups with or without RuN_4-SAzyme (n = 7 per group). WBC: white blood cells, RBC: red blood cells, PLT: platelets, MCV: mean corpuscular, MCHC: mean corpuscular hemoglobin concentration, MCH: mean corpuscular hemoglobin, HGB: hemoglobin, HCT: hematocrit. Data are presented as means ± SEM.

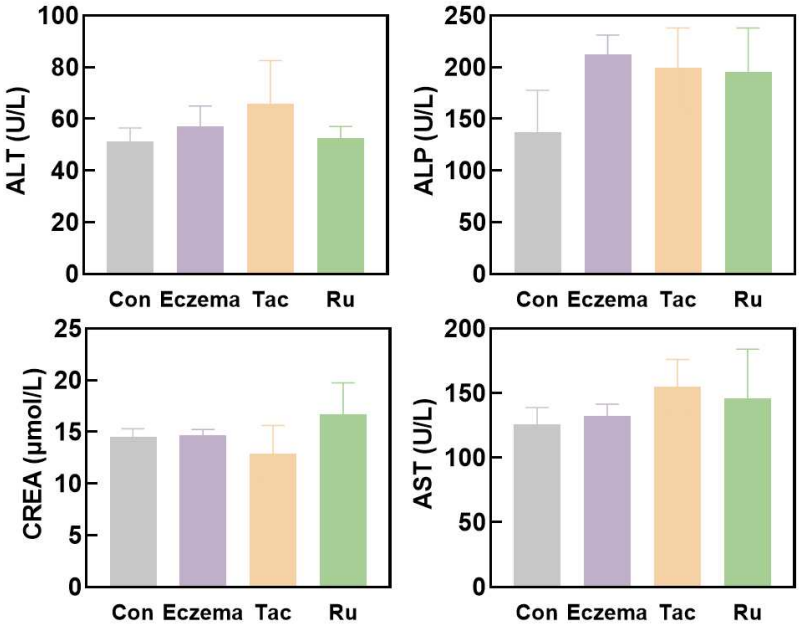

Fig. S14 Hematology data of mice in groups with or without RuN_4-SAzyme (n = 7 per group). ALT: Alanine aminotransferase, ALP: Alkaline phosphatase, CREA: Creatinine, AST: Aspartate transaminase. Data are presented as means ± SEM.

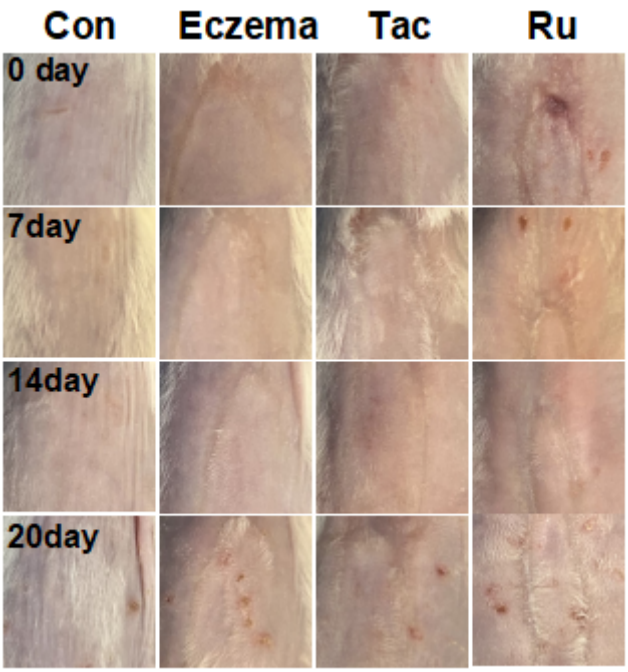

Fig. S15 Photographs of the backs of mice with or without intervention on the 0, 7, 14 and 20 days after treatment.

Supplementary Table S1. Comparison of the kinetic parameters between RuN_4-SAzyme and other single-atom nanozymes towards the TMB and H_2O_2 substrates during the POD-mimic catalysis. [1-7]

Enzyme	Substance	K_m (mM)	Reference
RuN_4-SAzyme	TMB	0.077	**This work**
	H_2O_2	16.09	
MoSA-N_3-C	TMB	0.79	*Chem. Soc. Rev.*, 2021, **50**,
	H_2O_2	2	7436
ZnN_4 SAEs	TMB	0.224	*Angew. Chem. Int. Ed.* ,
	H_2O_2	40.16	2019, **58**, 4911
Ru/CDs SAE	TMB	0.22	*ACS Appl. Mater. Inter.*
	H_2O_2	0.146	2021, **13**, 45269.
Fe-N_5	TMB	0.652	*Adv. Mater.* 2022. **34**.
	H_2O_2	11.2	2107088.
FeBNC	TMB	2.22	*Nano Today* 2020, **35**,
	H_2O_2	25.24	100971.
CeN_4-$SAzyme_{800/0.1}$	TMB	1.65	*Nano Today* 2024, 56,
	H_2O_2	18	102236.
pero-nanozysome	TMB	0.18	*Adv. Funct. Mater.*
	H_2O_2	175.5	2020,**31**,2007130.

Reference:

1. Q. Chang, J. Wu, R. Zhang, S. Wang, X. Zhu, H. Xiang, Y. Wan, Z. Cheng, M. Jin, X. Li, P. Xu, F. Jin and J. Wang, *Nano Today*, 2024, **56**, 102236.
2. C. Jiang, H. Huang, X. Kang, L. Yang, Z. Xi, H. Sun, M. D. Pluth and L. Yi, *Chem. Soc. Rev.*, 2021, **50**, 7436-7495.
3. L. Jiao, W. Xu, Y. Zhang, Y. Wu, W. Gu, X. Ge, B. Chen, C. Zhu and S. Guo, *Nano Today*, 2020, **35**, 100971.
4. W. Wang, Y. Zhu, X. Zhu, Y. Zhao, Z. Xue, C. Xiong, Z. Wang, Y. Qu, J. Cheng, M. Chen, M. Liu, F. Zhou, H. Zhang, Z. Jiang, Y. Hu, H. Zhou, H. Wang, Y. Li, Y. Liu and Y. Wu, *ACS Appl. Mater. Interfaces*, 2021, **13**, 45269-45278.
5. J. Xi, R. Zhang, L. Wang, W. Xu, Q. Liang, J. Li, J. Jiang, Y. Yang, X. Yan, K. Fan and L. Gao, *Adv. Funct. Mater.*, 2021, **31**, 2007130.
6. B. Xu, S. Li, L. Zheng, Y. Liu, A. Han, J. Zhang, Z. Huang, H. Xie, K. Fan, L. Gao and H. Liu, *Adv. Mater.*, 2022, **34**, 2107088.
7. B. L. Xu, H. Wang, W. W. Wang, L. Z. Gao, S. S. Li, X. T. Pan, H. Y. Wang, H. L. Yang, X. Q. Meng, Q. W. Wu, L. R. Zheng, S. M. Chen, X. H. Shi, K. L. Fan, X. Y. Yan and H. Y. Liu, *Angew. Chem. Int. Ed.* , 2019, **58**, 4911-4916.